

Evaluation of soil liquefaction potential with a holistic approach: a case study from Araklı (Trabzon, Turkey)

A.E. BABACAN¹ and S. CEYLAN²

¹ Department of Geophysics Engineering, Karadeniz Technical University, Trabzon, Turkey

² Siyavuşpaşa Neighborhood, Barbaros Street, 3rd Street, Celal, İstanbul, Turkey

(Received: 5 February 2020; accepted: 18 May 2020)

ABSTRACT This study focuses on demonstrating how a holistic approach based on geophysical, geotechnical, and Artificial Neural Network (ANN) methods in a region where urban development is intense will crucially contribute to the assessment of liquefaction potential. The liquefaction potential of the coastal part of the Araklı district of Trabzon has been evaluated. First, earthquake scenarios for different magnitudes, which may affect the study area, were produced. Maximum acceleration values to use in liquefaction analysis were calculated from the scenarios. Second, geophysical data were collected using seismic refraction, multichannel analysis of surface waves, electrical resistivity tomography, and ambient vibrations measures. In addition, results of standard penetration test were taken from the drillings in the region. The liquefaction potential using these data was also determined by ANN. The results show that the studied area has a serious risk of liquefaction and the more reliable liquefaction estimates are performed in the study area with the holistic approach. The results of this study will be of great importance for taking necessary measures in constructing engineering projects in the region, especially along the coastline.

Key words: Trabzon, liquefaction potential, geophysical methods, artificial neural network.

1. Introduction

Earthquakes throughout human history were one of the most destructive natural disasters that threaten human life and structures. One of the most crucial physical events in soil due to an earthquake is liquefaction, which damages or destroys structures built on loose and saturated deposits. Liquefaction can cause serious damage such as collapsing or sinking in engineering structures. Determining the liquefaction hazard in the areas where there is an earthquake hazard is of great importance for proper planning by the civil engineers.

Turkey is in a seismic region due to tectonic and structural properties and many earthquakes have occurred throughout history. A number of 53 earthquakes with $M_s \geq 6.0$ and 15 earthquakes with $M_s \geq 7.0$ have occurred since 1903 in Turkey (URL-1, 2019). Liquefaction disasters were first recorded in the 1992 Erzincan earthquake in Turkey (Kayabasi and Gokceoglu, 2018). However, liquefaction has also occurred during many earthquakes in the past. The best example is the earthquake on 17 August 1999 in the Marmara region (Ansal *et al.*, 1999). In Turkey, many researchers have investigated liquefaction phenomena in different regions with different methods

(Sonmez and Ulusay, 2008; Uyanık *et al.*, 2013; Kayabasi and Gokceoglu, 2018). The analysis of soil liquefaction can be conducted using different techniques such as standard penetration test (SPT) (Seed and Idriss, 1971; Tunusluoglu and Karaca, 2018), cone penetration test (CPT) (Robertson and Campanella, 1985; Moss *et al.*, 2006; Papathanassiou *et al.*, 2015), and shear wave velocity (V_s) (Andrus and Stokoe, 2000; Youd *et al.*, 2001). Apart from these, ambient vibrations and artificial neural network techniques have begun to be used in liquefaction analysis in recent years (Huang and Tseng, 2002; Beroya *et al.*, 2009; Rezaei and Choobbasti, 2014; Abbaszadeh Shahri, 2016). The primary purpose of this paper is analysing the liquefaction potential using geophysical data. Liquefaction is one of the most important soil problems occurring in sandy and non-plastic silty soils. It is known that liquefaction does not occur in all soil layers. For this reason, first of all, it is necessary to examine the existence of geological conditions necessary for liquefaction and to determine the horizontal and vertical continuity of the layers with liquefaction potential. The main advantage of non-destructive geophysical methods with respect to CPT and SPT is the ability to provide data both vertically and horizontally in the same measurement. Moreover, geophysical methods could be used for estimation of liquefaction resistance in areas where CPT and SPT tests cannot be performed. Another purpose is to perform liquefaction analysis using the Artificial Neural Network (ANN) method.

The liquefaction potential of the studied area is investigated in detail. For this purpose, seismic refraction tomography (SRT), multichannel analysis of surface wave (MASW), ambient vibrations (HVSr) and electrical resistivity tomography (ERT) measurements were taken in the coastal area of Trabzon city, Araklı district in the eastern Black Sea region (Fig. 1a). The investigated area is located east of Trabzon and 30 km away from the city centre. Since Trabzon and its surroundings have not been considered as a high-risk area for earthquakes until recently, studies on liquefaction in this region are very limited.

2. Geological setting and seismicity

The eastern Pontides, lying in the E-W direction parallel to the Black Sea coast, belong to the Sakarya zone described by Okay and Tüysüz (1999). Eastern Pontides represent an old island arc and has been divided into different zones according to its tectonic, magmatic, and sedimentological characteristics by many researchers (Arslan *et al.*, 1997; Şen *et al.*, 1998). The eastern Pontides were divided into two sections as northern and southern zones by Özsayar *et al.* (1981), whereas Bektaş *et al.* (1995) and Eyuboglu *et al.* (2006, 2007) divided them into three sections as northern, southern, and axial zones.

Under the influence of the Alpine orogenic movements, different deformation structures in Trabzon and its surroundings (northern zone of the eastern Pontides) have developed among which vertical faults are controlling the tectonic development of NE, NW, and E-W directions of Trabzon and its surroundings. The presence of reverse faults covering the entire southern coast of the Black Sea is known from the TPAO/BP Eastern Black Sea Project Study Group (1997) seismic surveys and previous studies in this region (Nikishin *et al.*, 2003; Eyuboglu *et al.*, 2011) (Figs. 2a and 2b). In recent years, earthquake activity has increased in this region and many minor earthquakes have occurred (URL-2, 2017; URL-3, 2017) (Fig. 2c). In addition, the earthquake hazard map of Turkey, as recently proposed by the Disaster and Emergency Management



Fig. 1 - Location (a) and simplified geological map (b) of the studied area (modified from Güven, 1993).

Presidency of Turkey, prescribes a high seismic hazard for the Trabzon province. The province of Trabzon is about 110 km from the North Anatolian Fault, which is one of the most important active tectonic structures. A major earthquake at that fault could seriously affect the study area. Major and devastating earthquakes have happened at the fault in the past. The most important of these occurred in 1939 and 1992 with magnitude of 7.9 (M_s) and 6.8 (M_s), respectively (URL-1,

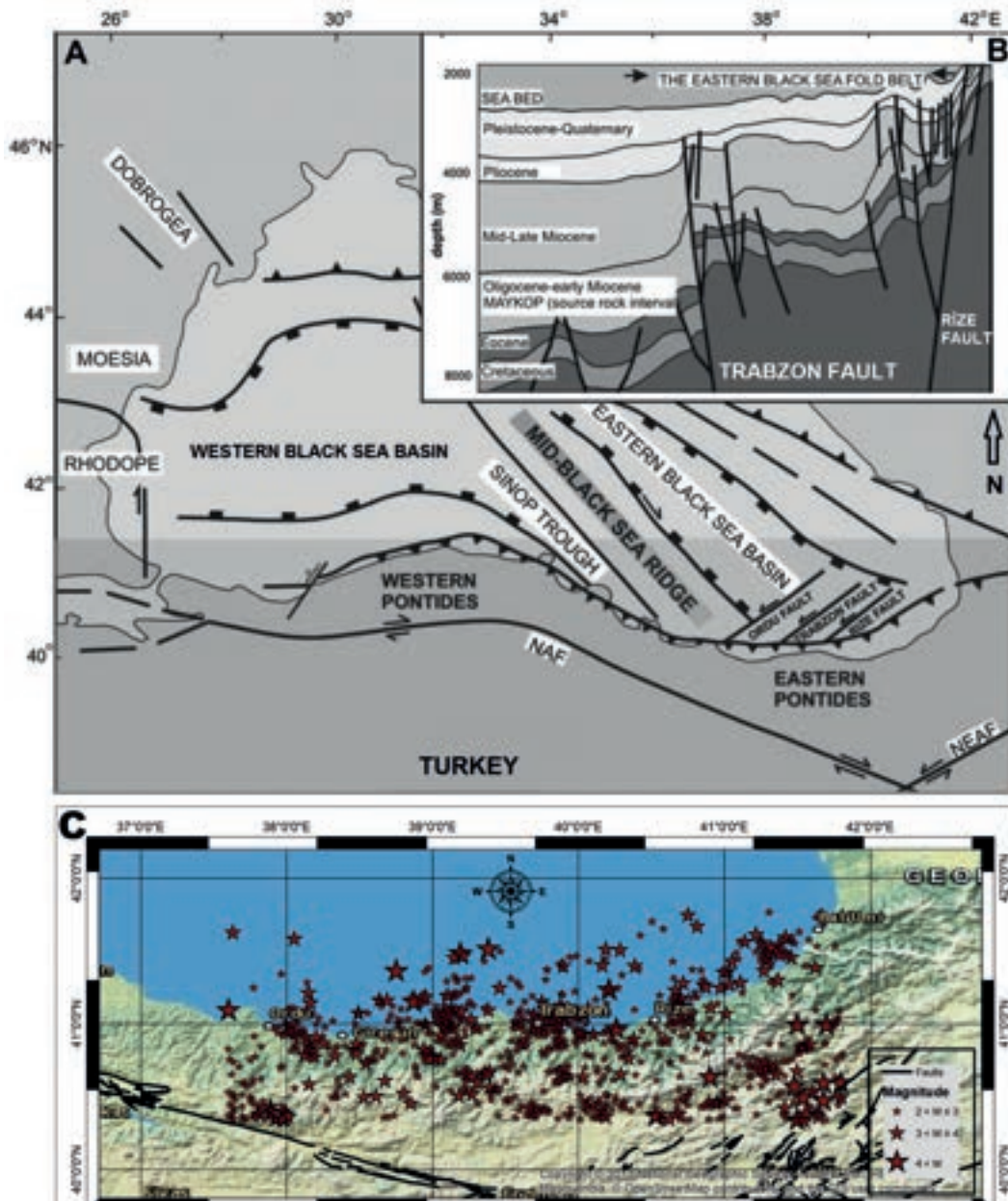


Fig. 2 - Tectonic map (panels a and b) covering Black Sea and its surrounding (TPAO/BP Eastern Black Sea Project Study Group, 1997; Eyüboğlu *et al.*, 2011) and epicentre map (c) in the region (Emre *et al.*, 2013; URL-2, 2017; URL-3, 2017).

2019). After the earthquake of 1992, there has been no earthquake larger than magnitude 6.0 in this region (URL-4, 2019). The region between Tokat and Erzincan has a high seismic activity and the probability of a magnitude 7.8 earthquake in the next 100 years is 90% (Bayrak and Türker, 2017). Considering the distance to this region, a similar earthquake can seriously affect the study area and its surroundings. There are three different formations in the study area (Fig.

1b), which is located in the northern zone of the eastern Pontides. The turbiditic facies sediments, underlying the volcanic and volcano-sedimentary units in and around Trabzon city, were referred to as Bakırköy Formation by Güven (1993). The unit is composed of clayey-sandy limestone, marl, claystone and, to a lesser extent, sandstone intercalations, and forms vast outcrops around the Taşönü region of the study area. The formation is overlain by Eocene aged units with an angular unconformity, and its age is determined as Late Cretaceous-Paleocene according to the fossil content (Güven, 1993). Giving extensive outcrops in the study area, the Eocene Kabaköy Formation (Güven, 1993) starts with clastic sediments and passes to volcanic rocks towards upper zones. The formation is composed of andesite, basalt, and pyroclastic rocks, which are intercalated by sandstone, sandy limestone, and marl. The yellowish, fossiliferous sedimentary rocks below the dark volcanic rocks act as an age guide level. The age of the formations is determined to be Early-Middle Eocene thanks to this guide layer (Güven, 1993). In the study area, especially near and south of the Araklı town centre outcrops, the unit is composed of pebble stone, sandstone, claystone, and alluvium. The alluvium in the riverbeds is relatively young. Alluvials are generally trapped in narrow valleys in the eastern Black Sea region. For these reasons, their width is commonly less than 50 m and thickness of 10-40 m. These alluvials contain groundwater, which is fed by surface water. In general, liquefaction potential does not turn into a risk since there is no settlement on alluvial terrains. However, especially in Araklı district, there is a dense settlement standing on these loose sediments that have a thickness of more than 30 m on the coast. These areas carry the risk of liquefaction. The groundwater depth is approximately 3 m. According to the drillings, the subsoil consists of alluvial deposits (sand size materials) down to 15 m depth, while geophysical measurements document a thickness of >30 m. The soil materials of the studied area were classified according to the Unified Soil Classification System (USCS) (ASTM D2487-11, 2011) in the SP and SM classes.

3. Geophysical methods

Integrated geophysical methods can provide more accurate and detailed information in the analysis of liquefaction potential. To evaluate the liquefaction hazard of the study area, SRT, MASW, ERT, and HVSR measurements were acquired by geophysical methods and parameters to be used for liquefaction calculation were determined. All geophysical measurements were carried out on the Quaternary deposits. Moreover, the acceleration value to be used in the liquefaction calculation was determined from the peak ground acceleration map created by taking into account the worst earthquake scenario (Fig. 3a). Earthquake magnitude with regard to this scenario was taken as $M_s = 7.9$. This was the largest earthquake in Erzincan and its vicinity in the last century. The peak ground acceleration values were mapped using the empirical formula proposed by Ambraseys *et al.* (1996). In addition, a map of the macroseismic intensity that can be observed in and around the studied area during the same earthquake was prepared (Fig. 3b). The formula given by Erdik and Eren (1983) was used in the calculation of the intensity values.

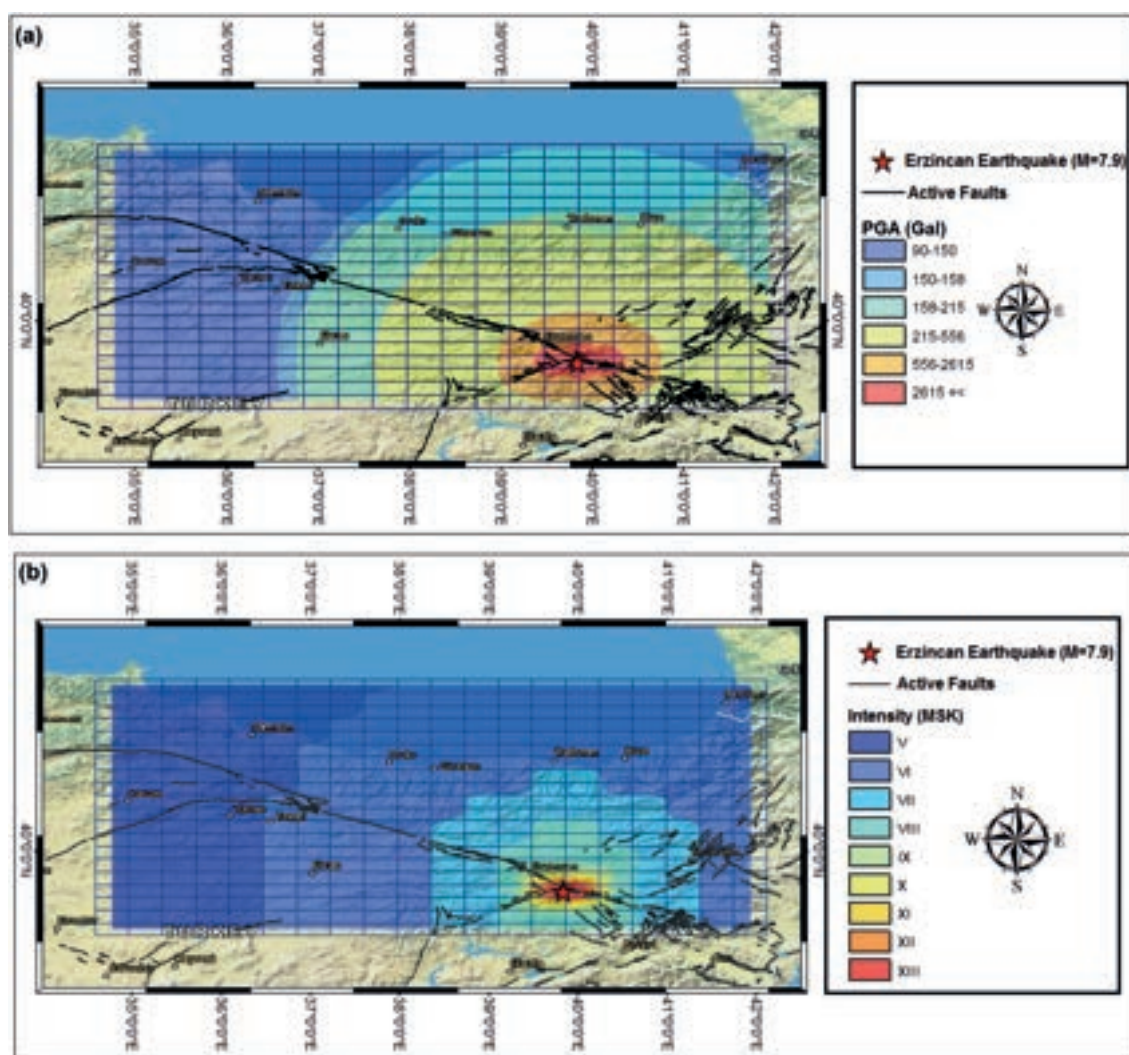


Fig. 3 - Peak ground acceleration (a) and macroseismic intensity maps (b) for the study area and its surroundings for the scenario earthquake ($M = 7.9$) (ESRI, 2017; URL-1, 2019).

4. Electric resistivity tomography

The electrical resistivity method reveals the underground structures by sending current into the ground by current electrodes and measuring voltage differences at potential electrodes. The main objective is to determine the change in groundwater level, water flow regime, and bedrock topography. However, the electrical resistivity method has a very effective and widespread use in determining the permeability, humidity, salinity, space and degree of decomposition, lithological changes in lateral and vertical directions, fault and fracture systems (Reynolds, 1997). ERT measurements use a combination of many potential and current electrodes connected to a multi-cable system. This system is placed on the ground at certain intervals along a survey line and measurements are made automatically. In this study, it is aimed to obtain information about the groundwater level, geological structure, and material. Furthermore, the depth of the groundwater

level inferred from ERTs was used in the liquefaction analysis. ERT data were collected with a Wenner-Schlumberger array, using 41 electrodes in 6 profiles. The electrodes spacing for six profiles were 3.0, 2.0, 1.5, 2.5, 2.5, and 2.0 m, respectively (Fig. 4). The apparent resistivity data were collected with an ABEM Terrameter LS and the data were inverted by using the Res2Dinv program (Geotomo, 2009). The current intensity was adjusted between 5 and 200 mA and the ABEM Terrameter LS automatically adjusts the selected current intensity range. 2D ERT images



Fig. 4 - Location of ERT profiles, seismic profiles, and ambient vibration measurements. The geometric scheme of the measurement profiles for SRT and MASW are given at the lower left corner.

of the studied area are shown in Fig. 5, where the iteration numbers and RMS error rates can be seen. In 3 of the 6 ERT profiles, the RMS error rates are above 10%. It is thought that the reason for the error rates being greater than 10% is not due to low quality data. The variation percentages of the measured values are also low. Moreover, all data points were checked in the Res2Dinv program, and the outliers were removed before the inversion of apparent resistivity data. This is probably because there is a large difference between the minimum and maximum of apparent resistivity values measured. The measured, calculated, and inverse model for the ERT section (5th profile), with the highest error rate, is given in Fig. 6. In addition, in Fig. 7, a linear regression graph for measured and calculated apparent resistivity for this section is given. A total of 464 apparent resistivity data is used for the inversion of this profile. The measured and calculated apparent resistivity values are compatible.

5. Seismic prospecting

SRT and MASW measurements were conducted along 8 profiles (Fig. 4) to calculate longitudinal (V_p) and shear wave (V_s) velocities and layered structure of underground in the

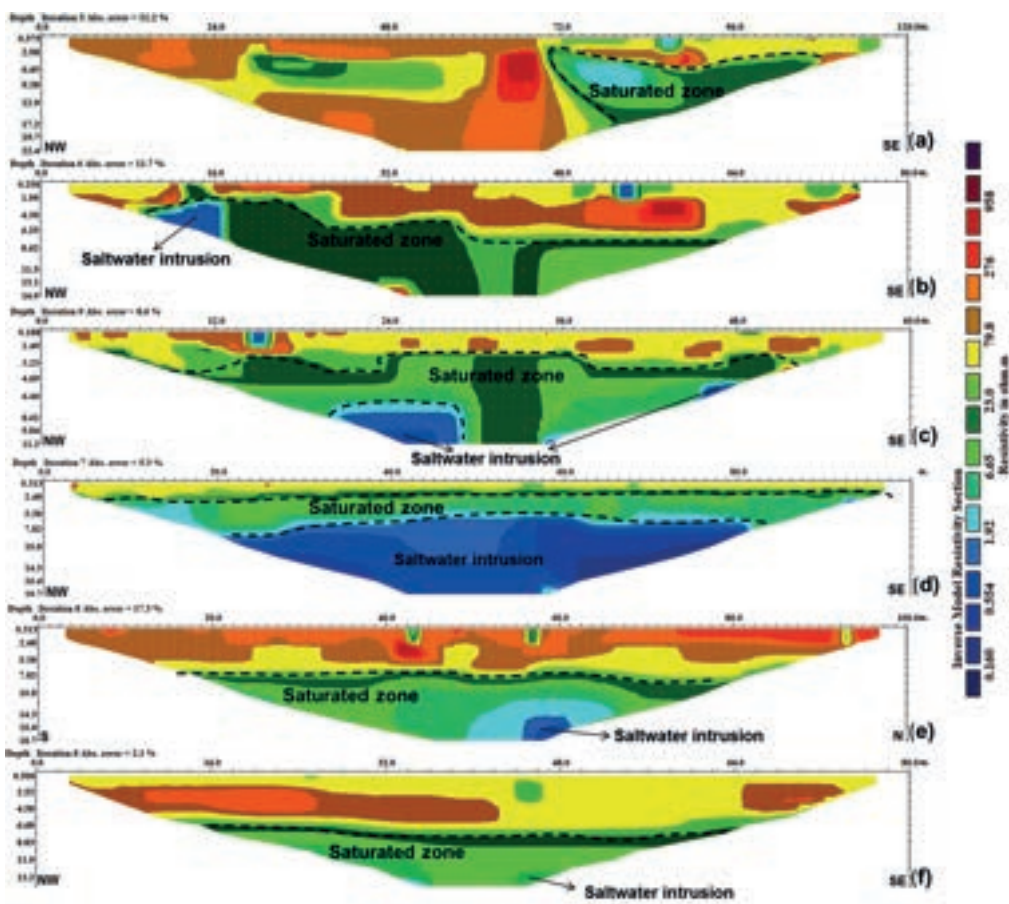


Fig. 5 - Results of ERT sections in the studied area: a) profile 1, b) profile 2, c) profile 3, d) profile 4, e) profile 5, f) profile 6.

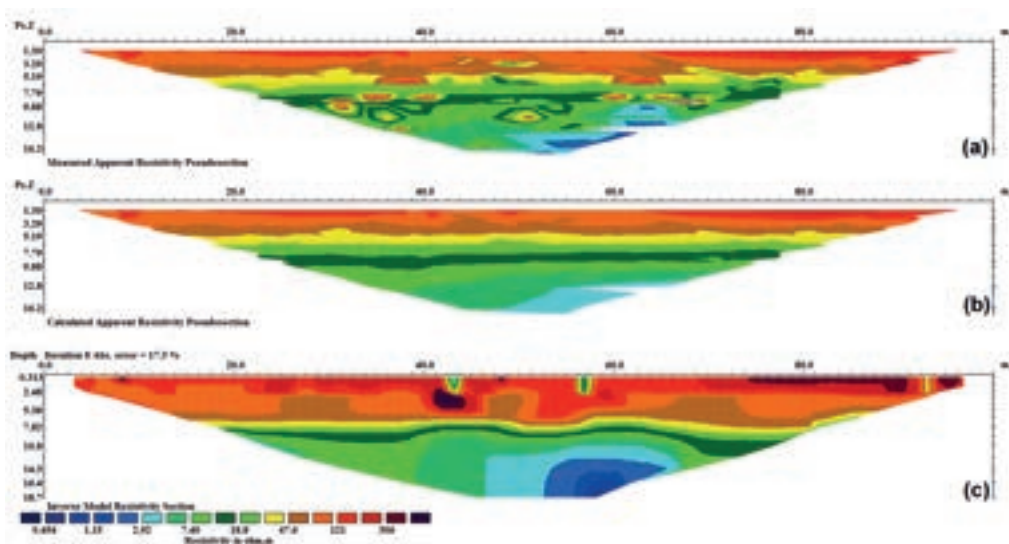


Fig. 6 - Measured apparent resistivity pseudo-section (a), calculated apparent resistivity pseudo-section (b), and inverse model resistivity section (c) for profile 5.

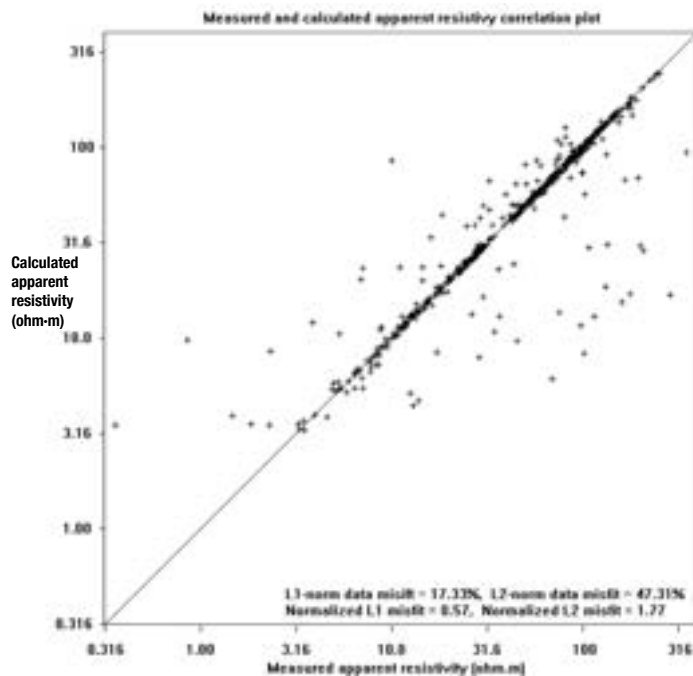


Fig. 7 - Measured and calculated apparent resistivity correlation plot for profile 5.

studied area. PASI 24-channel research seismograph was used in the seismic measurements. Twenty-four receivers with 4.5 Hz vertical components were used. The seismic source was a 10-kg sledgehammer and impact plate. Source locations and receivers were along a straight line. Seven shot points were used for each SRT profile. Many shots were done to enhance the signal-to-noise ratio (S/N) in each shot point. However, since the underground structure is composed of very loose and water-saturated material, reliable and quality data could not be obtained at far offset shot points of SRT measurements with a long profile. Therefore, these data were not used in SRT solutions. The source-receiver geometry for both SRT and MASW is given in Fig. 4 in detail. The signals were recorded for 0.25 s with sampling interval of 0.25 ms in SRT measurements. Time-distance graphs were drawn from the first arrival time of the seismic shot gather obtained from the seismic refraction method. 2D V_p cross-sections (Figs. 8 and 9) of the underground were obtained from the tomographic inversion solution of time-distance graphs, generally after ten or more iterations. The V_p velocity section for the profile 5 could not be obtained because a reliable first arrival time reading could not be performed. Only the V_s velocity section is calculated in this profile. Obtaining the tomographic velocity section from the seismic data for the first profile is shown in detail in Figs. 8a to 8c. In this study, the SeisImager/2D software was used for the tomographic inversion of seismic refraction data (Geometrics, 2009). This software uses a non-linear travel time technique (Hayashi and Takahashi, 2001). The tomographic inversion technique uses the simultaneous iterative reconstruction technique (SIRT) (Gilbert, 1972). SIRT is one of the prominent iterative reconstruction techniques (Lehmann, 2007). In Lehmann (2007) the mathematical formulations and detailed information about the SIRT technique are given. Tomographic inversion is an iterative technique: it is based on traveltimes calculation, initial velocity model constructions and minimisation of the difference among observed and calculated travel times (Bishop *et al.*, 1985).

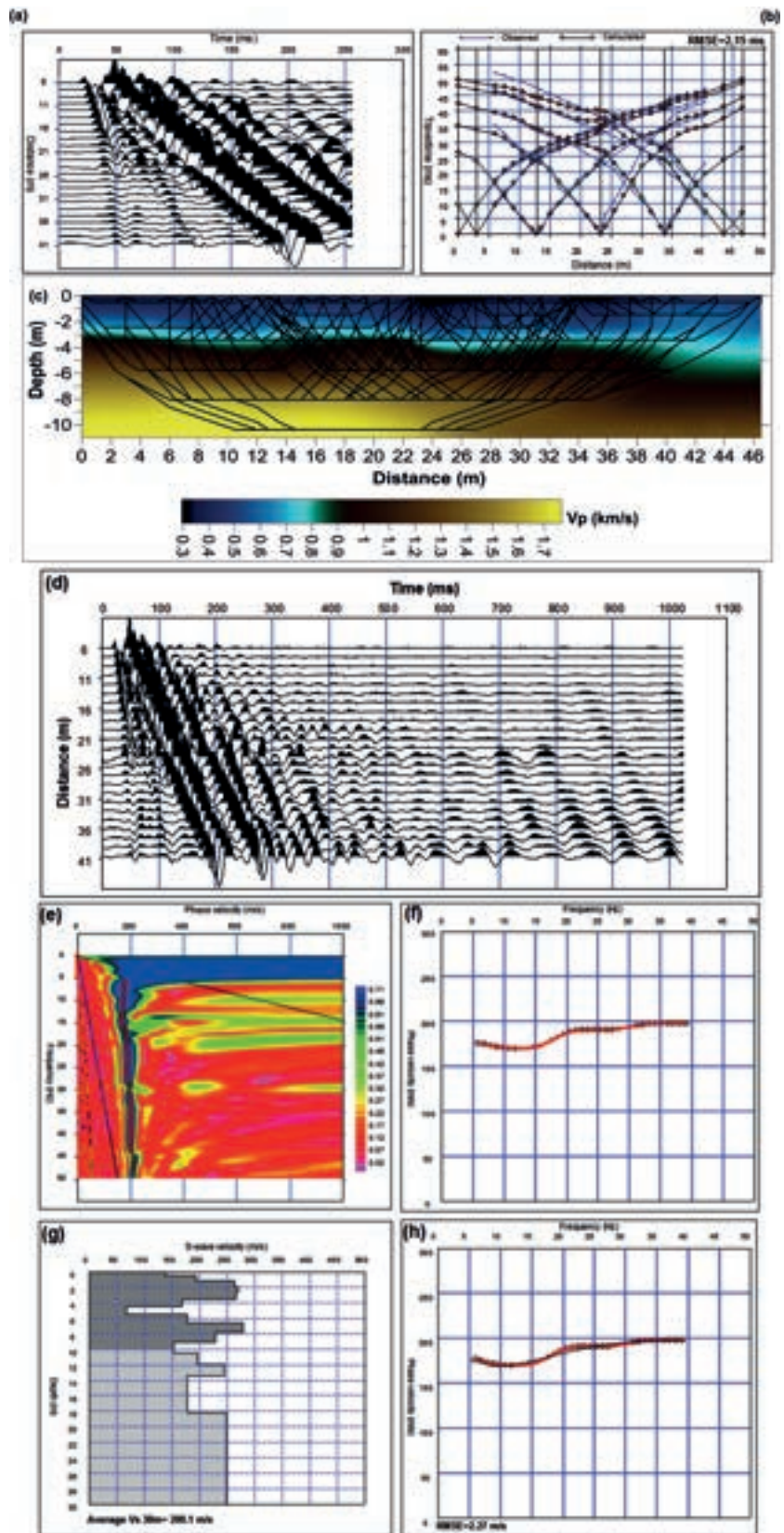


Fig. 8 - Results of SRT and MASW for the first profile in the studied area: a) seismic data for SRT, b) travel times-distance graphs and comparing of observed and calculated travel times, c) V_p tomographic section. Solid black lines show the raypath (d), seismic data for MASW (e), phase velocity vs. frequency (f), dispersion curve (g), 1D V_s profile (h) comparing of observed and calculated dispersion curves.

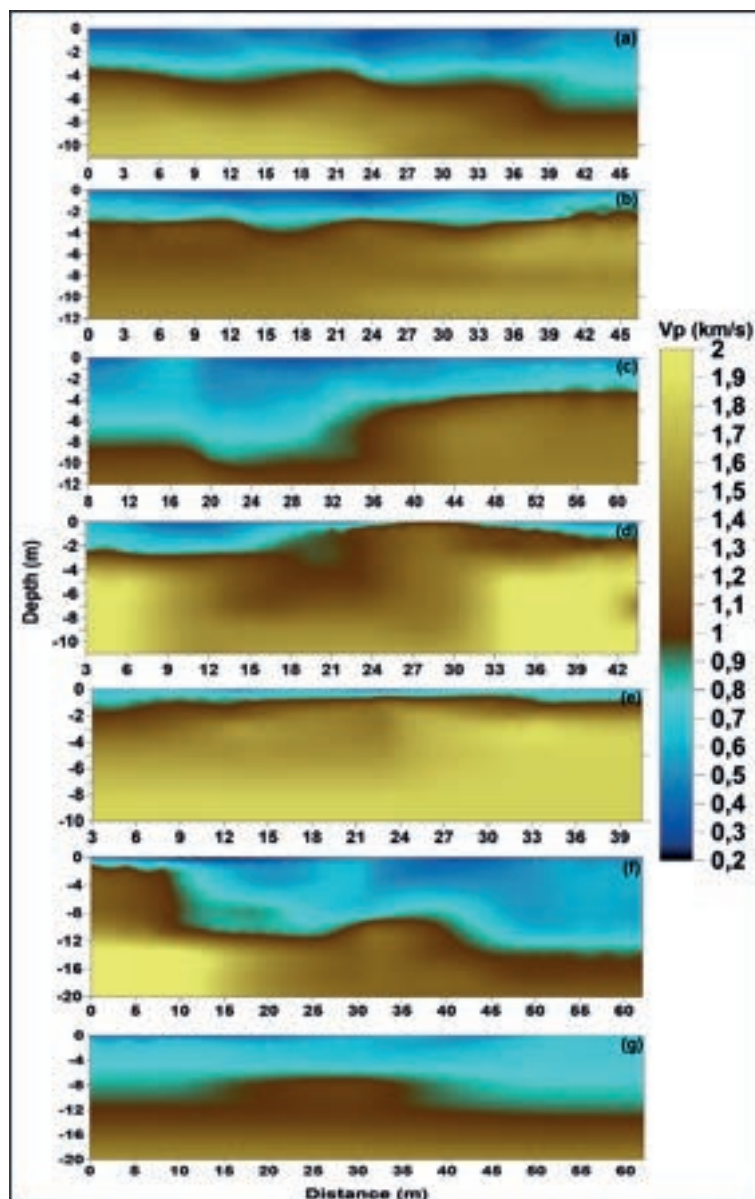


Fig. 9 - 2D V_p sections obtained from SRT measurements from the study area: a) profile 1, b) profile 2, c) profile 3, d) profile 4, e) profile 6, f) profile 7, g) profile 8.

V_s velocities used in both liquefaction analysis calculations and the determination of 1D underground structure were calculated by the MASW (Park *et al.*, 1999) method. MASW has been successfully applied in the identification of local site condition (Pischiutta *et al.*, 2017; Babacan *et al.*, 2018) and liquefaction analyses (Lin *et al.*, 2004; Uyanık *et al.*, 2013) for many years. In this method, the V_s velocities are basically determined by the dispersion properties of Rayleigh waves from the surface waves propagated in the layered media (Xia *et al.*, 2004). The determination of the V_s velocity in the MASW method consists of 3 stages. In the first stage, the seismic data (shot gathers) are collected in the field. Second, dispersion curves are created by Rayleigh waves. Dispersion curves are usually obtained by wavefield transformation techniques (Fourier, radon transform, phase shift, etc.). Dispersion curves were obtained by using the phase shift method

(Park *et al.*, 1998) in this study. Here, the dispersion curve is created by picking the maximum amplitude points on each frequency on the velocity spectrum by means of phase shift (Hayashi, 2008). At the last stage, one dimensional (1D) V_s images are calculated from the inversion of the dispersion curves. This process is an iterative solution. First, an initial model is defined by taking into account the surface wave velocity on the shot gather, the characteristic structure of the dispersion curve, and prior information. Then, V_s sections are obtained by applying the nonlinear least squares technique on the model (Hayashi, 2003). In this paper, MASW measurements were taken along 8 profiles. The source-receiver geometry for MASW is given in Fig. 4. The source locations were placed at 0 m (zero) and a forward shot was done. The source-receiver offset was chosen to be 4 times the receiver spacing. 3-5 vertical stacks are used to increase S/N during data acquisition. The signals were recorded for 1 s with a sampling interval of 1.024 ms in MASW measurements. The MASW data were analysed using the SeisImager software. Figs. 8d to 8g show the solution stages of MASW data in detail. The dispersion curves obtained by the MASW method show both normal and inverse dispersion properties. The parts where the velocity decreases with depth show inverse dispersion, and since these areas are saturated with water, V_s decreases with depth. 1D V_s sections are given in Figs. 8f and 10.

When V_s sections are examined, lateral variations are seen in some profiles. One of the main problems in the MASW method is the presence of lateral heterogeneities, which reduce the resolution of the survey (Dal Moro and Pipan, 2007). Depending on the lateral heterogeneity, the energy distribution between the different modes in surface wave analysis may not be the same across the entire frequency band (Foti *et al.*, 2018). In other words, the energy of the fundamental mode can be transferred to high modes in the presence of lateral variations. When the phase velocity frequency images obtained from the profiles with lateral variations are examined, the fundamental mode is clear, although some scatterings in energy distribution are observed. Moreover, the effects of lateral variations were examined by making both forward and reverse shots.

6. Ambient vibrations measurements

Local soil conditions have a great effect on the occurrence of liquefaction during an earthquake. For this reason, it is very important to correctly define the local soil conditions. Ambient vibration measurements (microtremor/HVSR) are one of the widely used non-destructive geophysical methods to determine local soil conditions (Nakamura, 1997; Bindi *et al.*, 2000; Babacan and Akın, 2018; Pamuk, 2019). With this method, the predominant frequency and amplification of the soil can be calculated and, then, soil classification can be carried out. Moreover, in recent years, many studies have been performed to assess the soil liquefaction potential using vulnerability index (K_g) calculated from microtremor data (Huang and Tseng, 2002; Beroya *et al.*, 2009; Rezaei and Choobbasti, 2014). Mokheri and Fard (2018) stated that the K_g value can be used as a parameter to evaluate the liquefaction potential of a soil. In this study, ambient vibration measurements were recorded at 14 points (Fig. 4) from west to east along on the coast of the Arakli district of Trabzon province to evaluate the potential of liquefaction of soil. Microtremor data were taken by a portable three-component digital broadband seismometer (Guralp System CMG-6TD). For quality data, the ME criteria (SESAME European Research Project WP12 Group, 2004) have been considered in measurements (Bard, 1999). The data obtained from HVSR can

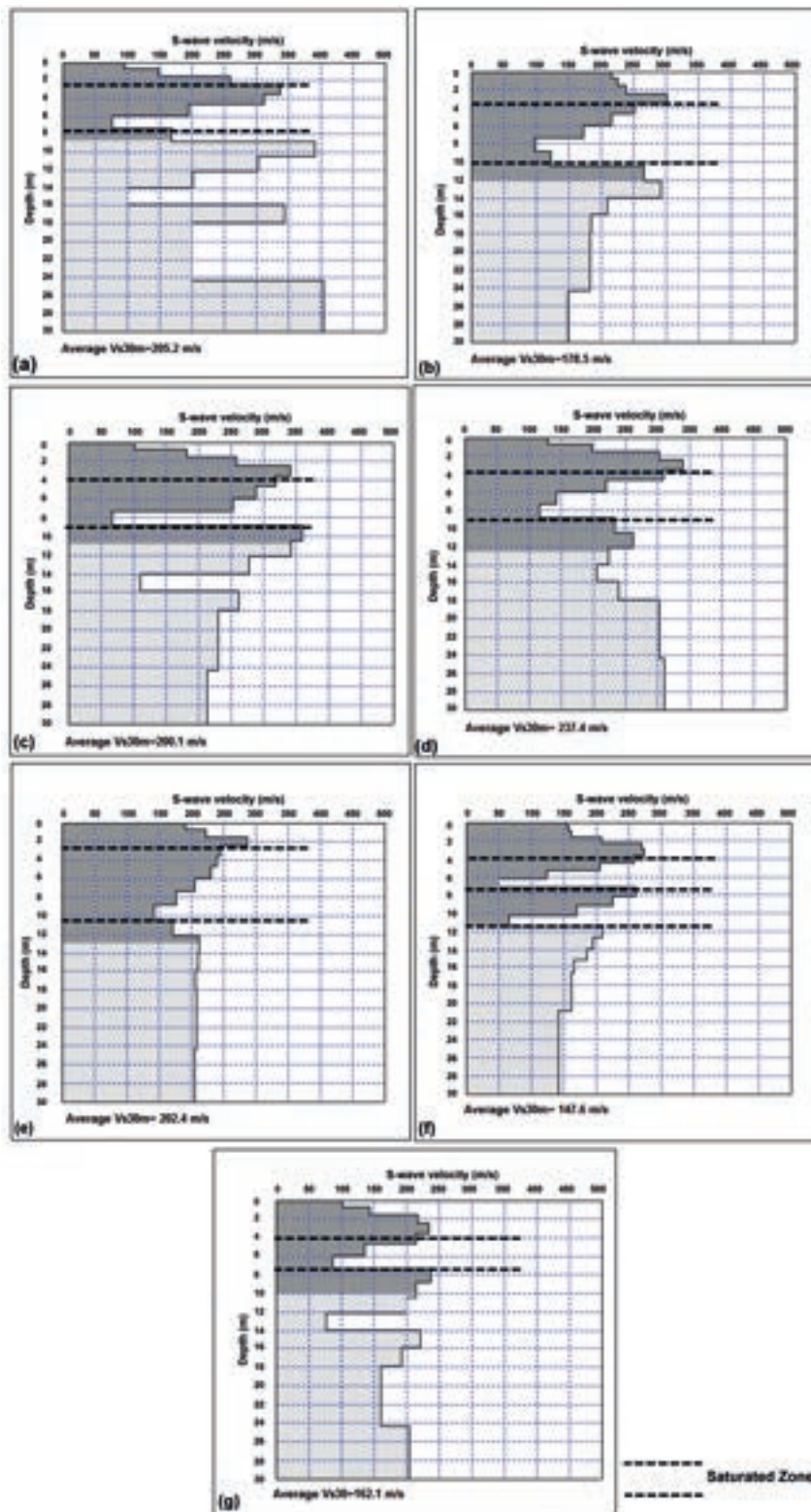


Fig. 10 - 1D V_s sections obtained by the MASW measurements for the study area: a) profile 2, b) profile 3, c) profile 4, d) profile 5, e) profile 6, f) profile 7, g) profile 8.

be analysed by many methods. One of the most common of these is the Nakamura H/V spectral ratio method which is fast and economical (Nakamura, 1989). Microtremor data were analysed using the Geopsy (www.geopsy.org) program for the H/V spectral ratio method. The predominant frequency and H/V ratio were determined by using the amplitude spectrum of three components. To obtain the H/V curve, a series of processes were applied to the data on the Geopsy program. The trend effect was removed by using the mean value from microtremor data. A band-pass filter from 0.5 to 20.0 Hz was applied, 25-s-long windows were selected and a 5% cosine window was applied to block energy leakage to data considering SESAME criteria. The Fast Fourier Transform (FFT) was performed in selected windows to obtain the amplitude spectra of three components of ground motion. The data were smoothed with a Konno-Ohmachi filter (Konno and Ohmachi, 1998) and the Bandwidth b -value of Konno-Ohmachi window was selected as 40. Finally, the horizontal/vertical (H/V) spectral ratios were obtained by using the geometric mean of the two horizontal E-W and N-S components. Data from 14 measurement points were evaluated using the Nakamura method and all results are presented in Fig. 11 and Table 1.

In recent years, the vulnerability index (K_g value) (Nakamura, 1996, 1997) which is calculated by using the amplification factor (A_g) and the predominant frequency (F_g) obtained from microtremor, can be used to evaluate the liquefaction potential:

$$K_g = A_g^2 / F_g. \quad (1)$$

If the K_g value is greater than 20, the soil is susceptible to high deformation (Nakamura, 1997). Huang and Tseng (2002) have used K_g values to estimate the soil liquefaction potential and the locations where K_g values are over 10 are risky areas for liquefaction. Rezaei and Choobbasti (2014) conducted a liquefaction assessment with traditional methods, artificial neural networks, and microtremor measurements in Iran in 2014 and compared the results. They calculated K_g

Table 1 - Parameters obtained from the HVSR measurements.

Measurement Points	Predominant Frequency (Hz)	Predominant Period (s)	H/V	Vulnerability (K_g value)
1	3.60	0.27	3.64	3.60
2	1.52	0.65	3.06	6.10
3	1.26	0.79	3.68	10.70
4	1.05	0.95	6.16	36.10
5	0.94	1.06	8.54	77.50
6	0.81	1.23	6.50	52.10
7	0.84	1.19	6.74	54.00
8	0.81	1.23	6.01	44.50
9	0.64	1.56	6.36	63.00
10	0.75	1.33	7.13	67.70
11	0.75	1.33	7.04	66.00
12	0.75	1.33	6.61	58.25
13	0.81	1.23	6.08	45.60
14	0.81	1.23	7.25	64.80

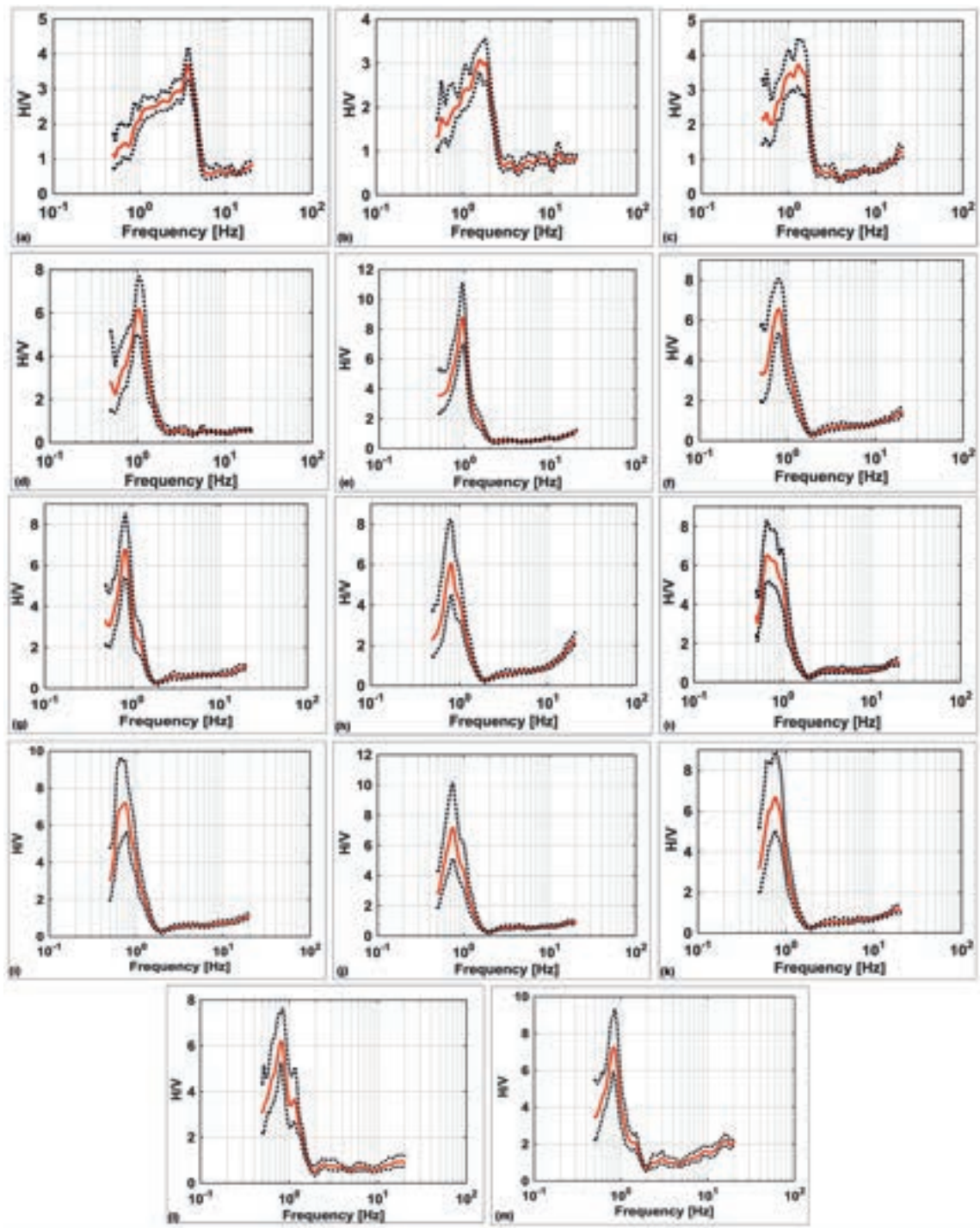


Fig. 11 - H/V spectra obtained from the ambient vibrations measurements. Letters from a to m correspond to microtremor measuring points from 1 to 14 in Fig. 4, respectively.

values from microtremor data and concluded that there is liquefaction potential when K_g is 5 or more. To evaluate the potential soil liquefaction of the study area, K_g values were calculated by Eq. 1 using amplification factor and predominant frequencies obtained from microtremor measurements collected at 14 points in this study. The results are given in Table 1.

7. Analysis of liquefaction using geophysical methods

There are various methods to determine liquefaction potential as proposed by various researchers: the simplified Seed and Idriss (1971) method, the method of initial acceleration (Dobry *et al.*, 1981), the periodic shear stress method (Seed and Idriss, 1981), and the liquefaction index method (Iwasaki *et al.*, 1984). In addition, the data obtained with in-situ tests, such as SPT, CPT, and V_s wave velocities determined by seismic methods, can be used to determine the liquefaction potential of soil. The Factor of Safety (FS) value against liquefaction is calculated using the data obtained in all of these methods and tests. Generally, there is liquefaction potential in case of $FS < 1$, but not in case of $FS > 1$. V_s are very advantageous because they can be obtained in all kinds of land conditions and in laboratories with lower costs than other methods. In this study, V_s velocities (Fig. 10) from MASW were used as the main method in liquefaction analysis. Moreover, 2D ERT sections and K_g (Nakamura 1996, 1997) values, obtained from microtremor measurements, were used in this study to evaluate the liquefaction potential. Liquefaction potential has been investigated in some studies by using the results obtained from the electrical resistivity method (Abu Zeid *et al.*, 2012; Giocoli *et al.*, 2014): from the resistivity distribution of the subsurface, saturated soil can be determined and the geological structure of the underground can be characterised. A safety factor (FS) is used to evaluate the potential liquefaction risk. FS vs. liquefaction is calculated as the ratio between the cyclic resistance ratio (CRR) and the cyclic stress ratio (CSR) (Seed and Idriss, 1971; Idriss and Boulanger, 2006). In addition, FS can be found by proportioning the shear stress ratio (SSR) to the shear resistance ratio (SRR) (Uyanık, 2006; Uyanık *et al.*, 2013). V_s velocities are taken into account in this formulation. Uyanık (2006) revealed a linear relationship between SSR and CSR . The formulations and other details of the method can be found in Uyanık *et al.* (2013). In this study, SRR and SSR were calculated by using the parameters obtained from geophysical methods and FS s were determined (Table 2). According to Iwasaki *et al.* (1981), the areas where FS is less than 1 indicate that the liquefaction hazard is high, and the areas greater than 1 indicate where the liquefaction hazard is low. Seed and Idriss (1982) found FS at 1.0 or below as liquefiable, among 1.0 and 1.2 as potentially liquefiable and upon 1.2 as non-liquefiable. In Table 2, values less than 1.0 are highlighted. FS values less than 1.0 in the table (including negative values), and corresponding depth (z) values, show liquefiable depths. Liquefiable depths generally vary between 6.0 and 13.5 m. As it can be seen, a significant part of the study area has a high liquefaction potential.

8. Analysis of liquefaction using artificial neural network

ANN is a method inspired by the human biological nervous system and has been successfully applied in the solution of complex engineering problems in recent years. ANN is formed by

Table 2 - Liquefaction analysis results for the Erzincan earthquake with $M_s = 7.9$. FS = safety factor, z = depth.

Seismic Profile	z (m)	FS	Seismic Profile	z (m)	FS	Seismic Profile	z (m)	FS
1	1.5	0.02900	4	1.5	-223.83900	7	1.5	-0.02838
1	3.0	0.22800	4	3.0	0.00547	7	3.0	0.34368
1	4.5	-0.06500	4	4.5	0.66243	7	4.5	0.61109
1	6.0	-0.76800	4	6.0	-710.73700	7	6.0	-0.13600
1	7.5	-1.50000	4	7.5	8.95989	7	7.5	-0.24137
1	9.0	-6.16400	4	9.0	8.47071	7	9.0	-2.06368
1	10.5	11.47700	4	10.5	6.79845	7	10.5	0.50671
1	12.0	6.11200	4	12.0	5.44842	7	12.0	0.21997
1	13.5	5.58100	4	13.5	1.64127	7	13.5	0.05861
2	1.5	-0.04700	5	1.5	-0.80824	8	1.5	-0.07325
2	3.0	0.56700	5	3.0	-0.35496	8	3.0	0.38844
2	4.5	0.30200	5	4.5	-1.23274	8	4.5	-0.06430
2	6.0	-2.72900	5	6.0	-46.1345	8	6.0	-0.33335
2	7.5	-2.84200	5	7.5	9.02305	8	7.5	-0.35824
2	9.0	-6.51600	5	9.0	7.41662	8	9.0	-0.14153
2	10.5	8.23700	5	10.5	6.97830	8	10.5	-0.08711
2	12.0	5.87600	5	12.0	5.64233	8	12.0	-0.62104
2	13.5	-1.01800	5	13.5	-0.36835	8	13.5	-1.29915
3	1.5	-2.25587	6	1.5	-0.41635			
3	3.0	1.25681	6	3.0	-0.99651			
3	4.5	-1.20900	6	4.5	-3.26348			
3	6.0	-1.41300	6	6.0	-85.97530			
3	7.5	16.69670	6	7.5	9.61716			
3	9.0	6.67092	6	9.0	6.29431			
3	10.5	6.67927	6	10.5	5.55054			
3	12.0	7.40939	6	12.0	5.52655			
3	13.5	-0.61115	6	13.5	-0.28582			

combining multiple neurons within certain categories. The main properties of the networks connecting the neurons are learning, memorising and determining the relationship between data. Generally, an ANN can be defined as a system consisting of a plurality of non-linear artificial cells that can be arranged in a single-layer or multi-layer and working in parallel (Nasr *et al.*, 2003). Essentially, neural networks are composed of three elements: neuron, the connection of the input-output vectors, and the weights of these connections (Elmas, 2003). The use of the ANN method in different areas of Earth sciences has increased in recent years (Gelisli *et al.*, 2015; Kilic and Eren, 2018). Moreover, many researchers have used the ANN method to evaluate liquefaction potential (Goh, 1996; Juang *et al.*, 2003; Rezaei and Choobbasti, 2014; Abbaszadeh Shahri, 2016).

FS with ANN using the MATLAB 2014 program (Demuth *et al.*, 2008) was determined. ANN can be trained to perform many complex functions. It uses various training algorithms to perform

these operations. In this study, a feedforward backpropagation algorithm was used as the artificial neural network type (Demuth *et al.*, 2008). Supervised training (Sathya and Abraham, 2013) was selected as a learning method. In this training algorithm, all activation functions were tried. The hyperbolic tangent sigmoid (de Harrington, 1993) was used as transfer function providing the best results. Moreover, models in the ANN structure are usually trained by the Levenberg-Marquardt algorithm (Marquardt, 1963; Hagan and Menhaj, 1994). Gradient descent with momentum back propagation algorithm was utilised as the learning rule; and the mean square error was utilised as the performance function. The training procedure is performed to minimise the difference between the estimated and the actual values. The parameters obtained from the experiments are inputs to an ANN model and, then, the results are estimated by various training algorithms and transfer functions in hidden layers. After that, the results are transferred to the output layer.

In this study, depth (z), magnitude (M_w), acceleration (a_{max}), stress reduction coefficient (rd), P-wave velocity (V_p), S-wave velocity (V_s), modulus of elasticity, shear modulus, Poisson ratio, and effective stress were used as input parameters in liquefaction analysis process with ANN. The number of training sets was 66 and the number of testing sets was 9. While training for each data set, the number of hidden layers, number of neurons in the hidden layer, degree of learning, momentum coefficient, and number of iterations were determined by trial and error. Data were normalised before analysis. The aim of normalisation is to ensure that the output parameter is between (+1) and (-1) for each parameter according to the minimum and maximum values. Thus, those taking the value of 1 in the output vector can be liquefied, while those taking the value of -1 are considered being non-liquefiable. Obtaining optimal results with ANN requires minimising the error. The error graphic of the artificial neural network selected for *FS* with a dependence on iteration is given in Fig. 12 and the epoch number where the training of models stopped was 4. Twenty neurons were used in this model. To check the accuracy of the network after the training, the network was tested with 9 data not used in the training. The results of ANN are shown in Fig. 13, including the number of neurons. The training step, the validation step, the test step and the average fit of these three steps are obtained as a percentage.

9. Results and discussion

In this paper, geophysical surveys and ANN were used to calculate the liquefaction potential of the studied area in Araklı district of Trabzon province. The properties of the soil were determined by the geophysical studies performed on the site and the previously drilling. The peak ground acceleration value used in the liquefaction analysis was based on the earthquake of magnitude 7.9 occurred on the North Anatolian Fault, which was the largest event in this region in the last century. The peak acceleration value (a_{max}) that may occur in the study area is approximately 0.22 g. According to the earthquake scenario, V_{S30} value is taken as 760 m/s for the soil conditions in the formulation used when calculating the peak acceleration value of the study area. Thereby, local ground conditions are not taken into account and local ground conditions should also be taken into account when calculating liquefaction. V_{S30} values calculated from MASW were found to be quite low in the study area. Considering this situation, it is inevitable that the peak acceleration value will be much larger in case of a large earthquake. This is also one of the reasons to increase the risk of liquefaction.

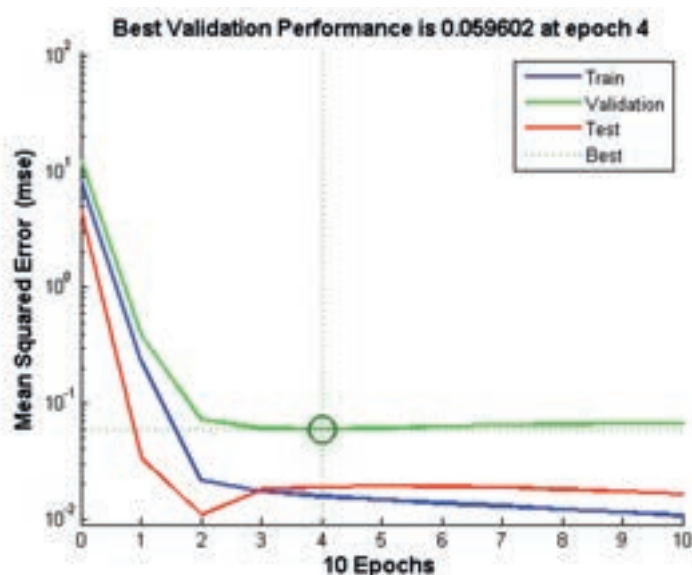


Fig. 12 - Graphic representation for the mean squared error variation of the ANN with dependence on iteration.

ERT measurements were conducted to determine the groundwater level, the depth of bedrock, and soil properties. The resistivity values range from about 0.2 to 800.0 ohm-m. Depending on the length of the profile in the ERT, information could be obtained between 11.0 and 22.4 m depth. In some of the ERT, although there are high resistivity values, these values do not indicate the presence of the bedrock. These higher values are mostly present in the first 5-6 m. Considering that the study area is a fill, these high values are mainly due to blocky rocks or voids (such as non-metallic wastewater pipes) in the soil embankment. According to the ERT, the groundwater level varies between about 2.5 and 6.5 m. Moreover, there is a saltwater intrusion in a major part of the study area.

Sensitivity of the V_s values obtained from the MASW measurements, correct determination of the largest peak ground acceleration, properties of the soil, and the magnitude of the earthquake are important factors for reliable liquefaction analysis. V_{s30} values obtained by using the MASW method in the study area generally varies between 150 and 240 m/s. However, the minimum and maximum V_s velocities for all profiles vary between 50 and 350 m/s. While the V_p velocities vary between 200 and 2100 m/s, the dominant velocity values are between 1500 and 1700 m/s. The groundwater level is between 3 and 6 m according to the MASW results. V_p sections support the results obtained from MASW. Both V_p and V_s indicate that the studied area is saturated with water and that the liquefaction potential is high.

According to the HVSR results, the natural frequency ranges from 0.64 to 1.52 Hz, and it is found to be 3.60 Hz only at the first measurement point. Although the frequency values in the study area are quite low, a high frequency value at the first measurement point can be thought of as a local effect. H/V values vary between 3.06 to 8.54 while K_g values vary also between 3.6 and 77.5 (Table 1). High K_g values were obtained in almost all of the study area. The higher the K_g value, the higher the probability of liquefaction potential. On the other hand, the K_g values in liquefied areas are higher than in neighbouring areas where no liquefaction occurs (Huang and Tseng, 2002). According to Nakamura (1997), Huang and Tseng (2002) and Rezaei and Choobbasti (2014), liquefaction potential hazard is high where the K_g values are greater than 20, 10 and 5, respectively.

According to the soil classification made by Kanai and Tanaka (1961), the soil class of the study area was defined as 4 (Z4). Class Z4 consists of soft delta deposits, alluvium containing mud, and topsoil units with a thickness of 30 m or more. The HVSR results are completely compatible with general geology.

According to the information obtained from the drillings with a depth of 15 m for different purposes in and around the study area in previous years, the study area is composed of alluviums (sand size materials). Drilling points are very close to the 5th-6th electrical and 7th-8th seismic measuring points. According to the drillings, the groundwater level is about 3 m and the SPT-N values vary between 10 and 25. According to the relative density and soil properties classification based on SPT-N values (Terzaghi and Peck, 1948), the relative density of the sands in the study area is loose and medium.

The evaluation of the liquefaction hazard of the study area was made using only the results obtained from the geophysical studies. The acceleration value was obtained from the earthquake scenario, the V_s velocities were obtained by the MASW method, and the groundwater level was obtained using both MASW and ERT methods. Other parameters are derived using this information. As can be seen from the Table 2 based on V_s velocity, the liquefaction potential is high in most of the coastal areas of the Araklı district of Trabzon city. It is observed that the potential of liquefaction in the eastern part of the area further increases.

In this study, FS values obtained for the liquefaction from experiments were also estimated with the ANN model. Considering the results obtained using the ANN method, the mean square error (MSE) was 0.05 at the 4 epoch (Fig. 10). When the performance evaluation criteria are considered, it is seen that the results are acceptable. According to the best MSE value in Fig. 12, the education of the network model (Training) was found as $R = 0.95$ and the test data (Test), which was not included in the training data and randomly selected, was found as $R = 0.94$ (Fig. 13). These results indicate that the model is well trained. Validation values and test data (Validation) were calculated as $R = 0.92$ and R value of all results (All) was calculated as 0.94 (Fig. 13). These results show that the network provides the approach to the estimation results at a high level of reliability.

10. Conclusion

Trabzon city constructions are usually built on the Black Sea coastal area due to its topography. The construction in the region is increasing day by day. According to the new earthquake hazard map prepared by the Disaster and Emergency Management Presidency of Turkey, Trabzon is one of the provinces with increased earthquake risk in Turkey. Moreover, in the next century there is a high probability of a major earthquake along the North Anatolian Fault, which is close to the province of Trabzon. For all these reasons, the potential liquefaction risk should be investigated in detail. Evaluation of liquefaction potential is vital in both field selection planning, and construction processes. In this study, more than one geophysical method (ERT, SRT, MASW, and HVSR) was used to evaluate the liquefaction potential. Liquefaction analysis was performed using only geophysical data without SPT and CPT data. Firstly, an evaluation was made using V_s velocities obtained from the MASW method. The groundwater level, which is one of the important parameters in the evaluation of the liquefaction potential, was determined from MASW

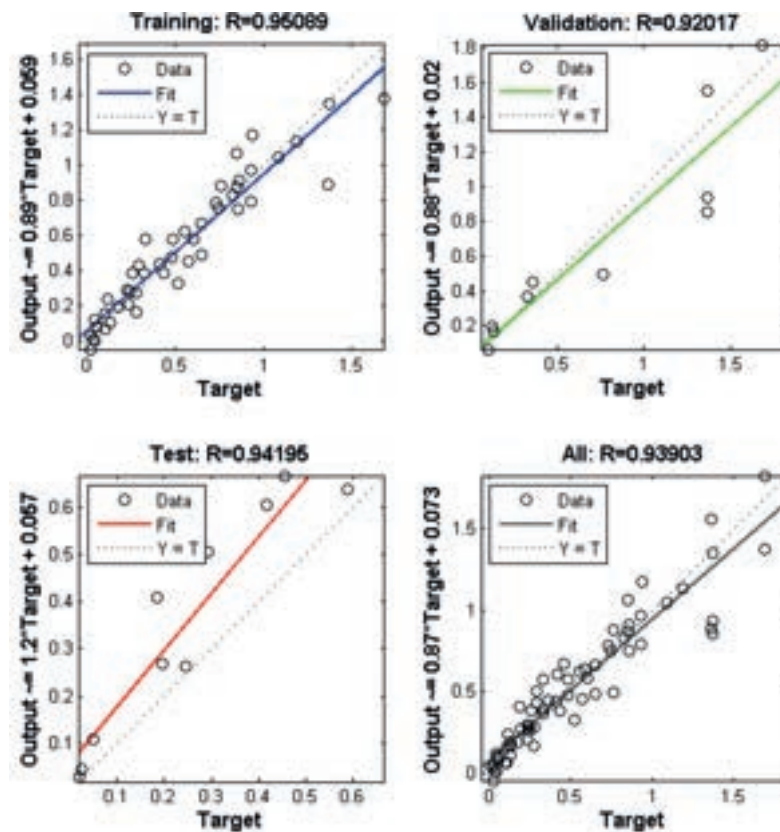


Fig. 13 - ANN performance outputs with a 20-neuron training set.

and ERT measurements. Then, an evaluation was also made by using the data obtained from the microtremor method which is used less in the literature to evaluate the liquefaction potential. Finally, a liquefaction analysis was carried out using the ANN method. The results obtained from all methods are quite compatible with each other. Moreover, in order to make comparisons, liquefaction analysis was carried out by using SPT-N values obtained from around 15 boreholes. The results obtained from SPT data were found to be consistent with the results obtained using V_s velocities.

Both V_p and especially V_s are quite low in the study area with V_s generally lower than 250 m/s. V_p values are usually lower than 2000 m/s. These velocities show that the studied area has a significant degree of liquefaction potential. ERTs show that the soil is saturated with water. Moreover, according to the K_g values obtained from microtremors, there is a serious potential of liquefaction, especially in the eastern parts of the study area. These results are also compatible with the results obtained from the liquefaction assessment with V_s velocity. In this area both the predominant period (max: 1.56 s) and H/V values (max: 8.54) are quite high. Therefore, the construction of multi-story buildings may be risky. Evaluation of liquefaction potential with the microtremor method can be a good preliminary assessment tool in terms of being fast and cheap. The liquefaction analysis using geophysical data was carried out without damaging the ground, in a shorter time and with less cost. The most important advantage of geophysical methods is the ability to collect data in both lateral and vertical directions in any environment. Thus, liquefaction analysis can be performed in any desired geological environment. In all soil

conditions, geophysical methods can be applied quickly, easily, and inexpensively, and the use of these methods in the liquefaction analysis is more advantageous than other methods.

Successful results were also obtained with ANN used in liquefaction analysis together with geophysical methods. It is seen that ANN can be applied to estimating *FS* successfully. *FS* can be calculated by using the ANN method with fewer parameters and in a shorter time within acceptable limits. Because many mathematical operations are performed in experimental calculations, an error may occur, but the probability of such an error in the ANN is very low.

According to the results obtained from all geophysical methods, there is a risk of liquefaction in a significant part of the study area. This risk is more increasing towards the east of the region. The evaluation of all the results obtained from geophysical methods with a holistic approach will reveal the liquefaction areas in a more detailed and safe manner. In addition, the results for the studied area will be helpful for geotechnical studies, earthquake and engineering geology. For this reason, a detailed liquefaction analysis should be carried out in Trabzon and the neighboring provinces before any construction and when necessary, soil remediation studies should be carried out before the construction.

Acknowledgements. The authors thank Daryl Tweeton for his help with the English of the final text. We also thank Hakan Ersoy for his helpful comments. We would like to thank editor and reviewers for their helpful suggestions and comments.

REFERENCES

- Abbaszadeh Shahri A.; 2016: *Assessment and prediction of liquefaction potential using different artificial neural network models: a case study*. Geotech. Geol. Eng., **34**, 807-815, doi: 10.1007/s10706-016-0004-z.
- Abu Zeid N., Bignardi S., Caputo R., Santarato G. and Stefani M.; 2012: *Electrical resistivity tomography investigation of coseismic liquefaction and fracturing at San Carlo, Ferrara Province, Italy*. Ann. Geophys., **55**, 713-716, doi: 10.4401/ag-6149.
- Ambraseys N.N., Simpson K.A. and Bommer J.J.; 1996: *Prediction of horizontal response spectra in Europe*. Earthquake Eng. Struct. Dyn., **25**, 371-400, doi: 10.1002/(SICI)1096-9845(199604)25:4<371::AID-EQE550>3.0.CO;2-A.
- Andrus R.D. and Stokoe K.H.; 2000: *Liquefaction resistance of soils from shear-wave velocity*. J. Geotech. Geoenviron. Eng., **126**, 1015-1025, doi: 10.1061/(ASCE)1090-0241(2000)126:11(1015).
- Ansal A., Bardet J.P., Bray J., Cetin O., Durgunoglu T., Erdik M., Kaya A., Ural D., Yilmaz T. and Youd T.L.; 1999: *Initial geotechnical observations of the August 17, 1999, Izmit earthquake*. Middle East Technical University, Earthquake Engineering Research Center, Ankara, Turkey, 68 pp., <nisee.berkeley.edu/turkey/report.html>.
- Arslan M., Tüysüz N., Korkmaz S. and Kurt H.; 1997: *Geochemistry and petrogenesis of the eastern Pontide Volcanic rocks, northeast Turkey*. Chemie der Erde., **57**, 157-187.
- ASTM D2487-11; 2011: *Standard practice for classification of soils for engineering purposes (unified soil classification system)*. ASTM International, West Conshohocken, PA, USA, 12 pp., doi: 10.1520/D2487-11.
- Babacan A.E. and Akın Ö.; 2018: *The investigation of soil-structure resonance of historical buildings using seismic refraction and ambient vibrations HVSR measurements: a case study from Trabzon in Turkey*. Acta Geophys., **66**, 1413-1433, doi: 10.1007/s11600-018-0208-0.
- Babacan A.E., Gelisli K. and Tweeton D.; 2018: *Refraction and amplitude attenuation tomography for bedrock characterization: Trabzon case (Turkey)*. Eng. Geol., **245**, 344-355, doi: 10.1016/j.enggeo.2018.09.008.
- Bard P.; 1999: *Microtremor measurement: a tool for site effect estimation?* In: Irikura K., Kudo K., Okada H. and Sasatani T. (eds), *The Effects of Surface Geology on Seismic Motion*, Balkema, Rotterdam, The Netherlands, pp. 1251-1279.
- Bayrak Y. and Türker T.; 2017: *Evaluating of the earthquake hazard parameters with Bayesian method for the different seismic source regions of the North Anatolian Fault zone*. Nat. Hazards, **85**, 379-401.

- Bektaş O., Yılmaz C., Taslı K., Akdağ K. and Özgür S.; 1995: *Cretaceous rifting of the eastern Pontide carbonate platform (NE Turkey): the formation of carbonates breccias and turbidites as evidences of a drowned platform*. Geol., **57**, 233-244.
- Beroya M.A.A., Aydin A., Tiglao R. and Lasala M.; 2009: *Use of microtremor in liquefaction hazard mapping*. Eng. Geol., **107**, 140-153, doi: 10.1016/j.enggeo.2009.05.009.
- Bindi D., Parolai S., Spallarossa D. and Cattaneo M.; 2000: *Site effects by H/V ratio: comparison of two different procedures*. J. Earthquake Eng., **4**, 97-113.
- Bishop T.N., Bube K.P., Cutler R.T., Langan R.T., Love P.L., Resnick J.R., Shuey R.T., Spindler D.A. and Wyld H.W.; 1985: *Tomographic determination of velocity and depth in laterally varying media*. Geophys., **50**, 903-923, doi: 10.1190/1.1441970.
- Dal Moro G. and Pipan M.; 2007: *Joint inversion of surface wave dispersion curves and reflection travel times via multi-objective evolutionary algorithms*. J. Appl. Geophys., **61**, 56-81.
- de Harrington P.B.; 1993: *Sigmoid transfer functions in backpropagation neural networks*. Anal. Chem., **65**, 2167-2168, doi: 10.1021/ac00063a042.
- Demuth H., Beale M. and Hagan M.; 2008: *Neural network toolbox™ 6. User's Guide*. The MathWorks Inc., Natick, MA, USA, 907 pp.
- Dobry R., Stokoe K.H., Ladd R.S. and Youd T.L.; 1981: *Liquefaction susceptibility from S-wave velocity*. In: Proc., ASCE National Convention, In Situ Tests to Evaluate Liquefaction Susceptibility, New York, NY, USA, Preprint 81-544, pp. 2-50.
- Elmas Ç.; 2003: *Yapay Sinir Ağları (Kuram, Mimari, Eğitim, Uygulama)*. Seçkin Yayıncılık, Baskı, Ankara, Turkey, pp. 65-90 (in Turkish).
- Emre Ö., Duman T.Y., Özalp S., Elmacı H., Olgun Ş. and Şaroğlu F.; 2013: *1/1.125.000 Ölçekli Türkiye Diri Fay Haritası*. Maden Tetkik ve Arama Genel Müdürlüğü Özel Yayınlar Serisi, Ankara, Turkey (in Turkish).
- Erdik M. and Eren K.; 1983: *Attenuation of intensities for earthquake associated with the North Anatolian Fault*. Middle East Technical University, Earthquake Engineering Research Center, Ankara, Turkey.
- ESRI; 2017: *ArcGIS Desktop 10.5.1*. Environmental Systems Research Institute, Redlands, CA, USA.
- Eyuboglu Y., Bektas O., Seren A., Maden N., Özer R. and Jacoby W.R.; 2006: *Three-directional extensional deformation and formation of the Liassic rift basins in the eastern Pontides (NE Turkey)*. Geol. Carpathica, **57**, 337-346.
- Eyuboglu Y., Bektas O. and Pul D.; 2007: *Mid-Cretaceous olistostromal ophiolitic mélangé developed in the back-arc basin of the eastern Pontide magmatic arc, northeast Turkey*. Int. Geol. Rev., **49**, 1103-1126, doi: 10.2747/0020-6814.49.12.1103.
- Eyuboglu Y., Santosh M., Bektas O. and Ayhan S.; 2011: *Arc magmatism as a window to plate kinematics and subduction polarity: example from the eastern Pontides belt, NE Turkey*. Geosci. Front., **2**, 49-56, doi: 10.1016/j.gsf.2010.12.004.
- Foti S., Hollender F., Garofalo F., Albarello D., Asten M., Bard P.Y., Comina C., Cornou C., Cox B., Di Giulio G., Forbriger T., Hayashi K., Lunedei E., Martin A., Mercerat D., Ohrnberger M., Poggi V., Renalier F., Sicilia D. and Socco V.; 2018: *Guidelines for the good practice of surface wave analysis: a product of the InterPACIFIC project*. Bull. Earthquake Eng., **16**, 2367-2420.
- Gelisli K., Kaya T. and Babacan A.E.; 2015: *Assessing the factor of safety using an artificial neural network: case studies on landslides in Giresun, Turkey*. Environ. Earth Sci., **73**, 8639-8646.
- Geometrics; 2009: *SeisImager/2D™ Manual, Version 3.3*. Geometrics Inc., San Jose, CA, USA, 257 pp.
- Geotomo; 2009: *Res2DInv ver. 3.59*. Geotomo Software, Gelugor, Penang, Malaysia, 151 pp.
- Gilbert P.; 1972: *Iterative methods for the three-dimensional reconstruction of an object from projections*. J. Theor. Biol., **36**, 105-117, doi: 10.1016/0022-5193(72)90180-4.
- Giocoli A., Quadrio B., Bellanova J., Lapenna V. and Piscitelli S.; 2014: *Electrical resistivity tomography for studying liquefaction induced by the May 2012 Emilia-Romagna earthquake (Mw = 6.1, northern Italy)*. Nat. Hazards Earth Syst. Sci., **14**, 731-737.
- Goh A.T.C.; 1996: *Neural-network modeling of CPT seismic liquefaction data*. J. Geotech. Eng., **122**, 70-73.
- Güven İ.H.; 1993: *Doğu Pontidlerin jeolojisi ve 1/250.000 ölçekli kompilasyonu*. MTA Yayınları, Ankara, Turkey, 65 s (in Turkish).

- Hagan M.T. and Menhaj M.B.; 1994: *Training feedforward networks with the Marquardt algorithm*. IEEE Trans. Neural Networks, **5**, 989-993, doi: 10.1109/72.329697.
- Hayashi K.; 2003: *Data acquisition and analysis of active and passive surface wave methods*. SAGEEP 20 Short Course, San Antonio, TX, U.S.A., 106 pp.
- Hayashi K.; 2008: *Development of surface-wave methods and its application to site investigations*. 京都大学 Kyoto University, Kyoto, Japan, 315 pp., doi: 10.14989/doctor.k13774.
- Hayashi K. and Takahashi T.; 2001: *High resolution seismic refraction method using surface and borehole data for site characterization of rocks*. Int. J. Rock Mech. Min. Sci., **38**, 807-813.
- Huang H.C. and Tseng Y.S.; 2002: *Characteristics of soil liquefaction using H/V of microtremors in Yuan-Lin area, Taiwan*. Terr. Atmos. Ocean. Sci., **13**, 325-338.
- Idriss I.M. and Boulanger R.W.; 2006: *Semi-empirical procedures for evaluating liquefaction potential during earthquakes*. Soil Dyn. Earthquake Eng., **26**, 115-130.
- Iwasaki T., Tokida K. and Tatsuoka F.; 1981: *Soil liquefaction potential evaluation with use of the simplified procedure*. In: Proc., 1st International Conference on Recent Advances in Geotechnical Earthquake Engineering and Soil Dynamics, St. Louis, MO, USA, pp. 209-214.
- Iwasaki T., Arakawa T. and Tokida K.I.; 1984: *Simplified procedures for assessing soil liquefaction during earthquakes*. Int. J. Soil Dyn. Earthquake Eng., **3**, 49-58, doi: 10.1016/0261-7277(84)90027-5.
- Juang C.H., Yuan H., Lee D.H. and Lin P.S.; 2003: *Simplified cone penetration test-based method for evaluating liquefaction resistance of soils*. J. Geotech. Geoenviron. Eng., **129**, 66-80.
- Kanai K. and Tanaka T.; 1961: *On microtremors VIII*. Bull. Earthquake Res. Inst., **39**, 97-114.
- Kayabasi A. and Gokceoglu C.; 2018: *Liquefaction potential assessment of a region using different techniques (Tepebasi, Eskişehir, Turkey)*. Eng. Geol., **246**, 139-161.
- Kilic G. and Eren L.; 2018: *Neural network based inspection of voids and karst conduits in hydro-electric power station tunnels using GPR*. J. Appl. Geophys., **151**, 194-204.
- Konno K. and Ohmachi T.; 1998: *Ground-motion characteristics estimated from spectral ratio between horizontal and vertical components of microtremor*. Bull. Seismol. Soc. Am., **88**, 228-241.
- Lehmann B.; 2007: *Seismic travelttime tomography for engineering and exploration applications*. European Association of Geoscientists & Engineers (EAGE), Amsterdam, the Netherlands, 273 pp.
- Lin C.P., Chang C.C. and Chang T.S.; 2004: *The use of MASW method in the assessment of soil liquefaction potential*. Soil Dyn. Earthquake Eng., **24**, 689-698.
- Marquardt D.W.; 1963: *An algorithm for least-squares estimation of nonlinear parameters*. J. Soc. Ind. Appl. Math., **11**, 431-441.
- Mokhberi M. and Fard A.Y.; 2018: *Liquefaction hazard assessment using horizontal-to-vertical spectral ratio of microtremor*. J. Struct. Eng. Geotech., **8**, 31-44.
- Moss R.E.S., Seed R.B., Kayen R.E., Stewart J.P., Der Kiureghian A. and Cetin K.O.; 2006: *CPT-based probabilistic and deterministic assessment of in situ seismic soil liquefaction potential*. J. Geotech. Geoenviron. Eng., **132**, 1032-1051, doi: 10.1061/(ASCE)1090-0241(2006)132:8(1032).
- Nakamura Y.; 1989: *A method for dynamic characteristics estimation of subsurface using microtremor on the ground surface*. Railway Tech. Res. Inst., Q. Rep., **30**, 25-33.
- Nakamura Y.; 1996: *Real-time information systems for hazards mitigation*. In: Proc., 11th World Conference on Earthquake Engineering, Acapulco, Mexico, Paper n. 2134, 8 pp.
- Nakamura Y.; 1997: *Seismic vulnerability indices for ground and structures using microtremor*. In: Proc., World Congress on Railway Research, Firenze, Italy, pp. 1-7.
- Nasr G.E., Badr E.A. and Joun C.; 2003: *Backpropagation neural networks for modeling gasoline consumption*. Energ. Convers. Manage., **44**, 893-905.
- Nikishin A.M., Korotaev M.V., Ershov A.V. and Brunet M.F.; 2003: *The Black Sea basin: tectonic history and Neogene-Quaternary rapid subsidence modelling*. Sediment. Geol., **156**, 149-168.
- Okay A.I. and Tüysüz O.; 1999: *Tethyan sutures of northern Turkey*. In: Durand B., Jolivet L., Horvath F. and Seranne M. (eds), The Mediterranean basin: Tertiary extension within the Alpine orogen, Geol. Soc., London, Spec. Publ., n. 156, pp. 475-515, doi: 10.1144/GSL.SP.1999.156.01.22.

- Özsayar T., Pelin S. and Gedikoglu A.; 1981: Doğu Pontidler'de Kretase (Cretaceous in the eastern Pontides). Karadeniz Teknik Üniversitesi Yerbilimleri Dergisi, **1**, 65-114. (in Turkish) .
- Pamuk E.; 2019: *Investigation of the local site effects in the northern part of the eastern Anatolian region, Turkey*. Boll. Geof. Teor. Appl., **60**, 549-568.
- Papathanassiou G., Mantovani A., Tarabusi G., Rapti R. and Caputo R.; 2015: *Assessment of liquefaction potential for two liquefaction prone areas considering the May 20, 2012 Emilia (Italy) earthquake*. Eng. Geol., **189**, 1-16.
- Park C.B., Miller R.D. and Xia J.; 1998: *Imaging dispersion curves of surface waves on multi-channel record*. In: Expanded Abstracts, 68th SEG Annual International Meeting, New Orleans, LA, USA, 17, pp. 1377-1380, doi: 10.1190/1.1820161.
- Park C.B., Miller R.D. and Xia J.; 1999: *Multichannel analysis of surface waves*. Geophys., **64**, 800-808.
- Pischiutta M., Villani F., D'Amico S., Vassallo M., Cara F., Di Naccio D., Farrugia D., Di Giulio G., Amoroso S., Cantore L., Mercuri A., Famiani D., Galea P., Akinici A. and Rovelli A.; 2017: *Results from shallow geophysical investigations in the northwestern sector of the island of Malta*. Phys. Chem. Earth, **98**, 41-48.
- Reynolds J.M.; 1997: *An introduction to applied and environmental geophysics*. John Wiley and Sons Ltd, Chichester, England, 796 pp.
- Rezaei S. and Choobbasti A.J.; 2014: *Liquefaction assessment using microtremor measurement, conventional method and artificial neural network (Case study: Babol, Iran)*. Front. Struct. Civ. Eng., **8**, 292-307, doi: 10.1007/s11709-014-0256-8.
- Robertson P.K. and Campanella R.G.; 1985: *Liquefaction potential of sands using the CPT*. J. Geotech. Eng., **111**, 384-403, doi: 10.1061/(ASCE)0733-9410(1985)111:3(384).
- Sathya R. and Abraham A.; 2013: *Comparison of supervised and unsupervised learning algorithms for pattern classification*. Int. J. Adv. Res. Artif. Intell., **2**, 34-38.
- Seed H.B. and Idriss I.M.; 1971: *Simplified procedure for evaluating soil liquefaction potential*. J. Soil Mech. Found. Div., **ASCE 97**, 1249-1273.
- Seed H.B. and Idriss I.M.; 1981: *Evaluation of liquefaction potential sand deposits based on observation of performance in previous earthquakes*. In: Proc., ASCE National Convention, St. Louis, (MO), USA, pp. 481-544.
- Seed H.B. and Idriss I.M.; 1982: *Ground motion and soil liquefaction during earthquakes*. Earthquake Engineering Research Institute, University of California, Berkeley, CA, USA, Monograph Series, 134 pp.
- Şen C., Arslan M. and Van A.; 1998: *Geochemical and petrological characteristics of the eastern Pontide Eocene (?) alkaline volcanic province, NE Turkey*. Turkish J. Earth Sci., **7**, 231-240.
- SESAME European Research Project WP12 Group; 2004: *Guidelines for the implementation of the H/V spectral ratio technique on ambient vibrations measurements, processing and interpretation*. European Commission - Research General Directorate, Project n. EVG1-CT-2000-00026 SESAME, Bruxelles, Belgium, 62 pp.
- Sonmez B. and Ulusay R.; 2008: *Liquefaction potential at İzmit Bay: comparison of predicted and observed soil liquefaction during the Kocaeli earthquake*. Bull. Eng. Geol. Environ., **67**, 1-9.
- Terzaghi K. and Peck R.B.; 1948: *Soil mechanics in engineering practice, 1st ed.* Wiley Pubs, New York, NY, USA, 584 pp.
- TPAO/BP Eastern Black Sea Project Study Group; 1997: *A promising area in the eastern Black Sea*. Leading Edge, **16**, 911-916.
- Tunusluoglu M.C. and Karaca O.; 2018: *Liquefaction severity mapping based on SPT data: a case study in Canakkale City (NW Turkey)*. Environ. Earth Sci., **77**, 422, doi: 10.1007/s12665-018-7597-x.
- URL-1; 2019: <www.koeri.boun.edu.tr/sismo/2/deprem-bilgileri/buyuk-depremler/>, <www.koeri.boun.edu.tr/sismo/2/deprem-bilgileri/buyuk-depremler/>, (accessed 1.16.19).
- URL-2; 2017: <www.deprem.gov.tr/tr/depremkatalogutle>, <www.deprem.gov.tr/tr/depremkatalogu>, (accessed 8.18.17).
- URL-3; 2017: <udim.koeri.boun.edu.tr/zeqdb/>, <udim.koeri.boun.edu.tr/zeqdb/>, (accessed 8.18.17).
- URL-4; 2019: <www.koeri.boun.edu.tr/sismo/2/deprem-bilgileri/buyuk-depremler/>, <www.koeri.boun.edu.tr/sismo/2/deprem-bilgileri/buyuk-depremler/>, (accessed 1.29.19).
- Uyanık O.; 2006: *Sıvılaşır yada sıvılaşmaz zeminlerin yinelemeli gerilme oranına bir seçenek*. Dokuz Eylül Üniversitesi Mühendislik Fakültesi Fen ve Mühendislik Dergisi, **8**, 79-91 (in Turkish).

- Uyanik O., Ekinici B. and Uyanik N.A.; 2013: *Liquefaction analysis from seismic velocities and determination of lagoon limits Kumluca/Antalya example*. J. Appl. Geophys., **95**, 90-103.
- Xia J., Miller R.D., Park C.B., Ivanov J., Tian G. and Chen C.; 2004: *Utilization of high-frequency Rayleigh waves in near-surface geophysics*. Leading Edge, **23**, 753-759.
- Youd T.L., Idriss I.M., Andrus R.D., Arango I., Castro G., Christian J.T., Dobry R., Finn W.D.L., Harder L.F., Hynes M.E., Ishihara K., Koester J.P., Liao S.S.C., Marcuson W.F., Martin G.R., Mitchell J.K., Moriwaki Y., Power M.S., Robertson P.K., Seed R.B. and Stokoe K.H.; 2001: *Liquefaction resistance of soils: summary report from the 1996 NCEER and 1998 NCEER/NSF workshops on evaluation of liquefaction resistance of soils*. J. Geotech. Geoenviron. Eng., **127**, 817-833.

Corresponding author: Ali Erden Babacan
Department of Geophysics Engineering, Karadeniz Technical University
61080 Trabzon, Turkey
Phone: +90 462 377 3428; e-mail: a.babacan@ktu.edu.tr